PILRα and PILRβ have a siglec fold and provide the basis of binding to sialic acid

Qiong Lu[a,b,1], Guangwen Lu[a,1], Jianxun Qi[a], Han Wang[a,b], Yifang Xuan[c], Qihui Wang[a], Yan Li[a], Yanfang Zhang[d], Chunfu Zheng[e], Zheng Fan[a], Jinghua Yan[a], and George F. Gao[a,b,c,d,f,2]

[a]CAS Key Laboratory of Pathogenic Microbiology and Immunology, Institute of Microbiology, Chinese Academy of Sciences, Beijing 100101, China; [b]University of Chinese Academy of Sciences, Beijing 100049, China; [c]Research Network of Immunity and Health, Beijing Institutes of Life Science, Chinese Academy of Sciences, Beijing 100101, China; [d]Laboratory of Protein Engineering and Vaccines, Tianjin Institute of Industrial Biotechnology, Chinese Academy of Sciences, Tianjin 300308, China; [e]Institutes of Biology and Medical Sciences, Soochow University, Suzhou 215123, China; and [f]Office of Director-General, Chinese Center for Disease Control and Prevention, Beijing 102206, China

Edited by Gary H. Cohen, University of Pennsylvania, Philadelphia, PA, and accepted by the Editorial Board April 29, 2014 (received for review November 4, 2013)

Paired immunoglobulin-like type 2 receptor α (PILRα) and β (PILRβ) belong to the PILR family and are related to innate immune regulation in various species. Despite their high sequence identity, PILRα and PILRβ are shown to have variant sialic acid (SA) binding avidities. To explore the molecular basis of this interaction, we solved the crystal structures of PILRα and PILRβ at resolutions of 1.6 Å and 2.2 Å, respectively. Both molecules adopt a typical siglec fold but use a hydrophobic bond to substitute the siglec-specific disulfide linkage for protein stabilization. We further used HSV-1 glycoprotein B (gB) as a representative molecule to study the PILR–SA interaction. Deploying site-directed mutagenesis, we demonstrated that three residues (Y2, R95, and W108) presented on the surface of PILRα form the SA binding site equivalent to those in siglecs but are arranged in a unique linear mode. PILRβ differs from PILRα in one of these three residues (L108), explaining its inability to engage gB. Mutation of L108 to tryptophan in PILRβ restored the gB-binding capacity. We further solved the structure of this PILRβ mutant complexed with SA, which reveals the atomic details mediating PILR/SA recognition. In comparison with the free PILR structures, amino acid Y2 oriented variantly in the complex structure, thereby disrupting the linear arrangement of PILR residues Y2, R95, and W108. In conclusion, our study provides significant implications for the PILR–SA interaction and paves the way for understanding PILR-related ligand binding.

There are two members in the paired immunoglobulin-like type 2 receptor (PILR) family: PILRα and PILRβ (1). Both are expressed as a monomeric transmembrane protein with a single V-set Ig-like (IgV) extracellular domain (2). In the cytoplasmic tail, PILRα bears two immunoreceptor tyrosine-based inhibitory motifs that deliver inhibitory signals by recruiting SHP-1 and SHP-2, whereas PILRβ binds to the DAP-12 molecule bearing a tyrosine-based activation motif (ITAM) for transduction of activating signals (3). Several studies in mice showed that the former is always related to the inhibition of the immune system, whereas the latter plays pivotal roles in activating natural killer (NK) cells and dendritic cells (DCs) and is involved in the mass production of inflammatory factors during infection (4). In addition, a recent report also demonstrated that PILRα could function to regulate neutrophil infiltration via activation of integrins during inflammation (5). Reminiscent of these immune-modulation functions, both receptors are largely expressed on cells of the immune system, especially those of the myeloid lineage such as monocytes, DCs, and macrophages (6, 7). PILRβ is also abundantly expressed on NK cells (6).

To exert their regulatory functions, the PILR receptors require engagement of specific ligands via their extracellular domains. Mouse CD99 is the only identified ligand for PILRβ to date (8). However, a set of host molecules, including mouse CD99 (8), PILR-associating neural protein (9), neuronal differentiation and proliferation factor-1 (NPDC1) (7), and collectin-12 (7), can recognize PILRα, implicating important roles of PILRα in diverse processes. In addition to the natural host ligands, PILRα is also hijacked by some viruses, such as HSV-1 (10) and porcine pseudorabies virus (11), for cell entry. The viral surface glycoprotein B (gB) is shown to recognize PILRα and mediate the virus infection (10, 11). Elucidation of the mechanisms underlying these ligand–receptor interactions is important in understanding PILR-involved physiological processes. Current knowledge on these interactions, however, only indicates the involvement of sialic acid (SA) moieties residing on the ligand surface in PILR engagement (7, 8, 12). This character drew parallels between PILRs and siglecs, a family of SA-binding Ig-type lectins (13). Nevertheless, PILRs, unlike siglec molecules, are of low SA-binding avidity and fail to bind to single SA sugars in a glycan microarray (14). The molecular basis of the PILR–SA interaction is an interesting, yet unresolved, issue.

In this study, we first solved both PILRα and PILRβ structures, demonstrating that they have siglec-like folds but maintain protein stability by hydrophobic interactions, different from siglecs, which have disulfide bonds. We also developed a Biacore-based assay for quantitative calculations of the PILR–SA interaction based on HSV-1 gB protein. A triresidue motif consisting of Y2, R95, and W108 was identified as a key SA-binding site in PILRα, and a W108L substitution in the motif was

Significance

The paired immunoglobulin-like type 2 receptor α (PILRα) and β (PILRβ) are important surface molecules which, upon ligand binding, can deliver opposing signals to modulate the host immune responses. In this study, we elucidated the molecular basis on the ligand binding of PILRs by systematic structural and functional assays. Both PILRα and PILRβ show a typical siglec-like fold but exhibit variant binding avidities for sialic acid (SA). We further identified key residues responsible for SA binding and elucidated the atomic interaction details via a complex crystal structure. In conclusion, the SA recognition mechanism for the PILR receptors has been, for the first time to our knowledge, systematically investigated and clearly presented.

Author contributions: G.F.G. designed research; Q.L., H.W., Y.X., Q.W., Y.L., and Y.Z. performed research; C.Z. and Z.F. contributed new reagents/analytic tools; J.Q. collected data and solved structures; Q.L., G.L., J.Q., and J.Y. analyzed data; and G.L., J.Y., and G.F.G. wrote the paper.

The authors declare no conflict of interest.

This article is a PNAS Direct Submission. G.H.C. is a guest editor invited by the Editorial Board.

Data deposition: Crystallography, atomic coordinates, and structure factors have been deposited in the Protein Data Bank, www.pdb.org (PDB ID codes 4NFB for PILRα, 4NFC for PILRβ, and 4NFD for the PILRβ-mut/SA complex).

[1]Q.L. and G.L. contributed equally to this work.

[2]To whom correspondence should be addressed. E-mail: gaof@im.ac.cn.

This article contains supporting information online at www.pnas.org/lookup/suppl/doi:10.1073/pnas.1320716111/-/DCSupplemental.

shown to be responsible for the inability of PILRβ to interact with gB. We further reported a complex structure of SA bound to a PILRβ L108W mutant protein, thereby presenting the atomic details mediating the PILR–SA interaction.

Results

Both PILRα and PILRβ Have a Siglec Fold. We first solved the structure of PILRα at 1.6 Å resolution. The final model, which was refined to R_{work} = 0.1980 and R_{free} = 0.2249 (Table S1), contains residues L1 to T119 (numbering based on the mature protein) of the native PILRα sequence (NM_013439.2). The content of the asymmetric unit of the crystal is a monomer. Consistent with the categorization of PILRα into the single IgV superfamily, the solved structure comprises two antiparallel β-sheets formed by strands ABDE and A′CC′FG (G, G′), exhibiting the characteristics of an IgV-like fold (Fig. 1*A*). Different from the classical IgV domain, however, the G strand of PILRα is kinked in the middle, splitting into two short strands (G and G′) connected by a short linker. In addition, the IgV-specific disulfide bond is also missing in PILRα, with only a single cysteine residue (C94) situating on the F strand.

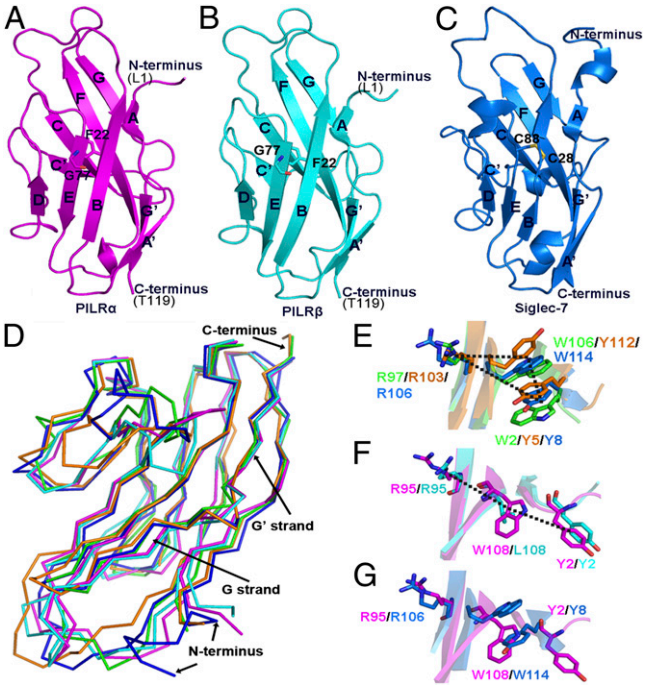

Fig. 1. Crystal structures of PILRα and PILRβ reveal a siglec fold. (*A–C*) Structures of PILRα in magenta (*A*), PILRβ in cyan (*B*), and siglec-7 (PDB ID code 1O7V) in blue (*C*) are depicted. F22 and G77, which form hydrophobic interactions in both PILR molecules, as well as C28 and C88, which form a disulfide bond in siglec-7, are shown in sticks. The β-strands in all structures are indicated with capitals. The terminal residues are marked in parentheses. (*D*) Superimposition of PILRα, PILRβ, siglec-1 (PDB ID code 1QFO), siglec-5 (2ZG2), and siglec-7 (1O7V) shown in a Cα ribbon representation and labeled in magenta, cyan, green, orange, and blue, respectively. The protein termini and the G, G′ strands are indicated. (*E–G*) A special linear arrangement of the Y2/R95/W(L)108 triresidue in PILRs. According to previous studies, the SA binding of siglecs involves three sterically proximate residues: an arginine and two aromatic amino acids. These three residues and their equivalent amino acids in PILRs are overlaid and shown as sticks. (*E*) An overlay of siglec-1 (W2, R97, and W106 in green), siglec-5 (Y5, R103, and Y112 in orange), and siglec-7 (Y8, R106, and W114 in blue). (*F*) An overlay of PILRα (Y2, R95, and W108 in magenta) and PILRβ (Y2, R95, and L108 in cyan). (*G*) An overlay of PILRα (Y2, R95, and W108 in magenta) and siglec-7 (Y8, R106, and W114 in blue). The steric arrangement of the triresidue is indicated with dotted lines.

The structure of PILRβ at 2.2 Å resolution was solved with an R_{work} = 0.2192 and an R_{free} = 0.2575 (Table S1). Two molecules related by a twofold axis are present in the asymmetric unit of the crystal. Overall, the two PILRβ protomers are of the same structure with an rmsd of only about 0.07 Å for all of the Cα pairs. Each molecule contains electron-density traceable residues from L1 to T119 (numbering based on the mature protein) of the native PILRβ sequence (NM_178238.2), folding into an IgV-like structure composed of the ABDE and A′CC ′FG(G,G′) sheets (Fig. 1*B*). As expected, this observed fold is very similar to that of PILRα described above. Superimposition of the two structures revealed that all of the scaffold strands and a majority of the intervening loops are well aligned, except for the BC and CC′ loops, which exhibit obvious conformational variance (Fig. S1).

Despite sharing low sequence identities (less than 25%) with siglecs (Fig. S2), PILRα and PILRβ display significant structural similarities to the siglec molecules (Fig. 1 *A–C*). For example, when superimposed, PILRα exhibits an rmsd of 1.3 Å over 91 Cα pairs to sialoadhesin (PDB ID code 1QFO), an rmsd of 2.3 Å over 84 Cα pairs to siglec-7 (PDB ID code 1O7V), and an rmsd of 2.6 Å over 96 Cα pairs to siglec-5 (PDB ID code 2ZG2) (Fig. 1*D*). According to a previous study (15), a kink of the G strand (into short G and G′ strands) was shown to be a conserved feature of siglecs, with which the G strand directly contacts the SA moiety and the GG′ loop accounts for ligand specificity. PILRα and PILRβ also contain this unique character. Hence, the PILR pairs strikingly adopt a typical siglec fold and preserve the structural features necessary for ligand interaction (Fig. 1 *A–D*).

Compared with canonical siglecs, however, the conserved intrasheet disulphide bond linking strands B and E is absent in PILRs. The corresponding positions are replaced with a phenyalanine residue (F22 in both PILRα and PILRβ) on strand B and a glycine residue (G77 in both PILRα and PILRβ) on strand E, which form hydrophobic interactions to stabilize the protein fold (Fig. 1 *A–C*).

Steric Arrangement of the Y2/R95/W(L)108 Triresidue in PILRs. The observation of an overall siglec fold for the PILR pairs urged us to further compare PILRs with siglecs for the steric arrangement of those residues identified as the key elements engaging SA. These include a conserved arginine residue (R97 in siglec-1, R103 in siglec-5, and R106 in siglec-7, numbering based on the mature proteins) situated in the middle of the F strand and two amino acids of less conservation but invariably aromatic side chains (W2 and W106 in siglec-1, Y5 and Y112 in siglec-5, and Y8 and W114 in siglec-7) located in the A and G strands, respectively (15–18). In siglecs, these three residues are sterically in close proximity, similarly positioned on the molecule surface, and arranged at the three points of an obtuse triangle (Fig. 1*E*). According to the previously reported siglec-7 structure in complex with a sialylated ligand GT1b, the arginine residue plays an indispensable role in SA binding by forming salt bridges with the SA carboxylate group. The two aromatic amino acids further facilitate the ligand interaction by providing hydrophobic and weak H-bond interactions (19).

In PILRs, amino acids Y2 in strand A, R95 in strand F, and W (L)108 in strand G (a tryptophan in PILRα and a leucine in PILRβ) are equivalent to the identified SA-binding triresidue of siglecs (Fig. S2). The three amino acids are spatially conserved between PILRα and PILRβ (Fig. 1*F*) but exhibit obvious variance in steric arrangement in comparison with siglec proteins (Fig. 1*G*). A detailed structure overlay using PILRα and siglec-7 as the representative revealed a well-aligned arginine residue but large conformational variances for the tyrosine and tryptophan residues between the two molecules. In PILRα, W108 rotates its indole ring ~90° toward strand A, thereby occupying the position initially taken up by Y8 of siglec-7. Consequently, PILRα extends its Y2 residue away from the protein main body, leading to an

overall linear arrangement of the Y/R/W triresidue (Fig. 1 *F* and *G*).

PILRα, but Not PILRβ, Binds HSV-1 gB Through SA. To further probe into the underlying molecular characters of PILRα and PILRβ we analyzed the SA-binding features of both proteins by surface plasmon resonance (SPR) using Biacore technology. According to previous studies, SA alone is not sufficient for any detectable PILR engagement (7, 14). We therefore resorted to the viral ligand of HSV-1 gB for the binding studies. The trimeric ectodomain protein of HSV-1 gB was prepared from either mammalian 293T cells (gB-293T) or insect Sf9 cells (gB-Sf9), and purified to homogeneity (Fig. S3). As expected, a clear interaction was observed when PILRα flew over immobilized gB-293T. The binding kinetics revealed a fast-on/fast-off mode, showing an affinity of ∼7 μM (Fig. 2*A* and Fig. S4). This specific interaction was dependent on the SA moieties, removal of which by treatment with neuraminidase (NA) was shown to largely attenuate the binding response (Fig. 2*E*). This result is also in good accordance with a previous cell-based assay (12). Moreover, we also tested gB-Sf9 in the same experiment. To our knowledge, the *O*-glycosylation in mammalian cells is largely different from that of Sf9 cells (Fig. 2*F*), which lacks SA transferase and thereby could not decorate proteins with sialylated sugar tips (20). Accordingly, no detectable binding could be observed between gB-Sf9 and PILRα (Fig. 2*E*). In conclusion, these results clearly demonstrated that PILRα relies on SA binding for a full capacity of gB engagement and validated the current SPR system (with immobilized gB-293T) as an effective method for studying PILR–SA interactions.

We then tested whether PILRα binding to SA involves the aforementioned Y/R/W triresidue in a manner similar to that in siglecs. The amino acid arginine was mutated to alanine, tyrosine to leucine, and the tryptophan residue was replaced with a leucine as in PILRβ, a gB nonbinder (21). The protein mutants were refolded and shown to behave similarly to wild-type PILRα in an analytical gel filtration assay (Fig. S5). In addition, none of the mutations interfered with the surface localization of PILRα (Fig. S6), indicating a proper folding of the PILR mutants. In the Biacore assay, both R95A (Fig. 2*B*) and W108L (Fig. 2*C*) mutations abrogated the binding between PILRα and gB-293T, whereas the Y2L substitution leads to an approximately twofold decrease in the binding affinity (∼14 μM) (Fig. 2*D*). The mutagenesis data demonstrate the functional importance of these three residues in ligand recognition.

Despite a high sequence identity (88%) between PILRα and PILRβ, the latter does not function as the HSV-1 receptor (21). Consistently, no obvious binding was detected between PILRβ (up to 12.5 μM) and gB-293T (Fig. 2*G*). We also tested by SPR the interaction between gB-293T and the PILRβ L108W mutant (PILRβ-mut). As expected, this mutant protein can be refolded (Fig. S5) and is observed to properly traffic to (Fig. S6) the cell surface as with wild-type PILRβ. The mutation confers a significantly elevated binding avidity to PILRβ, with a binding affinity of about 1 μM (Fig. 2*H*), confirming that L108 in PILRβ is responsible for SA nonbinding. Nevertheless, this restored gB-binding capacity does not suffice for PILRβ to mediate HSV-1 entry. Neither PILRβ nor PILRβ-mut was observed to facilitate the HSV-1 infection of CHO-K1 cells, in contrast to PILRα, which led to increased cell infection by the virus (Fig. S7).

Structural Basis of the PILR–SA Interaction. Despite great efforts, we failed to obtain any complex crystals of SA bound to PILRα. Instead, a cocrystal between PILRβ-mut and SA was successfully obtained by cocrystallization. The final structure, with a single SA moiety and a single PILR molecule in the asymmetric unit, was determined to 1.7 Å resolution and refined to $R_{work} = 0.1706$ and $R_{free} = 0.2117$ (Table S1). As expected, the L108W substitution did not change the overall structure of PILRβ. Superimposition of the wild type and the mutant structures yielded an rmsd of about 0.42 for 104 Cα pairs. The SA moiety is located on the lateral side of the IgV rear sheet in PILRβ-mut, perching on top of the G strand (Fig. 3*A*). In comparison with the free PILRα structure, the N-terminal loop and its residing Y2 residue oriented variantly in the complex structure. This resulted in a breaking of the linear arrangement of the Y/R/W triresidue as observed in the free PILR structures (Fig. S8), although it cannot be excluded that the variant conformation of Y2 in PILRβ-mut is related to the L108W mutation itself.

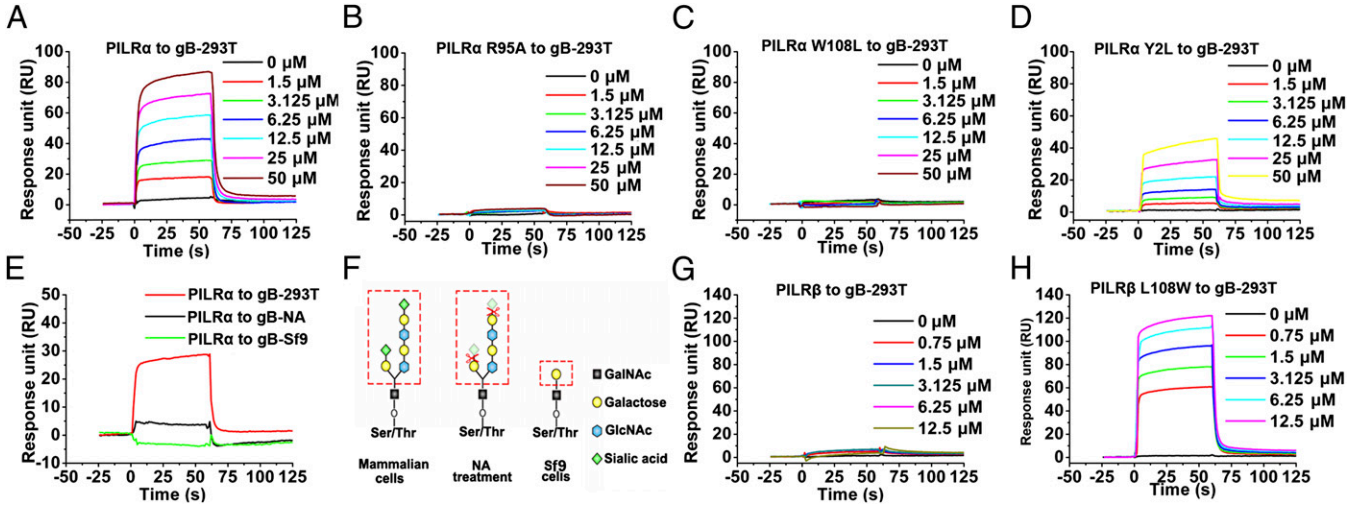

Fig. 2. SPR assays characterizing HSV-1 gB binding to PILRs and their mutants. Gradient concentrations of the indicated PILR proteins were passed over gB [gB-293T, gB-Sf9, or gB-293T treated with neuraminidase (gB-NA)] immobilized on a CM5 censor chip. The binding profiles are shown. (*A*) Wild-type PILRα to gB-293T. (*B*) PILRα R95A to gB-293T. (*C*) PILRα W108L to gB-293T. (*D*) PILRα Y2L to gB-293T. (*E*) Wild-type PILRα (3 μM) to gB-293T (red), gB-NA (black), and gB-Sf9 (green). (*F*) A schematic model showing the difference in *O*-glycosylation between 293T mammalian and Sf9 insect cells. The terminal of the glycan modification is always occupied by an SA moiety in mammalian cells (*Left*) but by a galactose or mannose in insect cells (*Right*). (*Center*) The NA cleavage of terminal SA moieties. (*G*) Wild-type PILRβ to gB-293T. (*H*) PILRβ L108W to gB-293T.

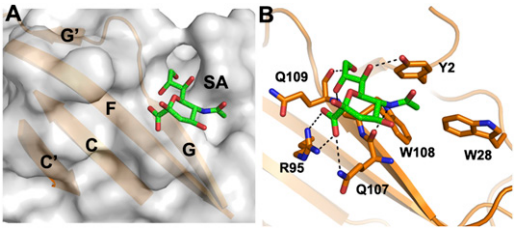

Fig. 3. Structural basis of the PILR–SA interaction. (*A*) The complex structure of SA bound to PILRβ-mut (L108W). The PILR protein is shown in surface, and the SA moiety in stick. Overall, SA is located on the lateral side of the PILR IgV rear sheet, which is highlighted as cartoons and labeled. (*B*) The atomic details mediating the PILR–SA interaction. The interface residues are shown as orange sticks and labeled and the SA moiety is presented in green. Dotted lines indicate H bonds or salt bridges.

We then characterized the atomic details at the binding interface. PILRβ-mut clamps SA in a shallow pocket centered on the G strand. The SA moiety runs its sugar ring in parallel over the pocket surface and orients its carboxylate and glycerol groups downward facing the protein main body. This allows the formation of a bundle of hydrophilic interactions between PILRβ-mut and SA to stabilize the binding. As for SA glycerol, this group was shown to simultaneously contact the main-chain groups of Q109 and the side chain of Y2 via H-bond interactions. The SA carboxylate group forms a salt bridge with the side chain of PILR residue R95 and simultaneously interacts with Q107 via an H bond (Fig. 3*B*).

The N-acetyl group of SA also contributes dramatically to the PILR–SA interaction. In the complex structure, the N-acetyl amide nitrogen was shown to form an H bond with the backbone oxygen of PILR Q107. In addition, the SA N-acetyl further appropriately positions its tip methyl group toward an apolar pocket formed by PILR residues Y2, W28, and W108, providing a strong hydrophobic interaction tying the sugar ligand with the protein receptor (Fig. 3*B*).

A Variant SA-Binding Mode in Comparison with Those Mediating Siglec–SA Interactions. We further compared our complex structure with previously reported structures of the siglec–SA complexes. Overall, the SA moiety adopts a similar orientation for protein engagement and occupies equivalent sites in the protein receptors. Nevertheless, the detailed atomic interactions in the binding site exhibit obvious differences between PILRβ-mut and siglecs, especially for the two aromatic amino acids of the key-binding triresidue. In siglecs, these two amino acids orient the side chains in a parallel manner, stacking against each other via a strong π–π interaction. This π–π unit lays beneath the SA moiety and hydrophobically interacts mainly with SA glycerol. In turn, the SA molecule flips its tip hydroxide in the glycerol group for solvent exposure (Fig. 4*A*). In PILRβ-mut, however, Y2 and W108 arranged their side chains almost perpendicularly. These two amino acids individually swung their side chains, relative to the corresponding residues in siglecs,~180° along the CA–CB axis, leading to the formation of a hydrophobic concave suitable for accommodation of the SA N-acetyl methyl. Without the limitation from the apolar contact as observed in siglecs, the glycerol group of SA orients its tip hydroxide downward for an H-bond interaction after PILR engagement (also discussed above in *Results*). It is interesting that the Y/R/W triresidue is also positioned triangularly in the PILRβ-mut–SA complex structure but mirroring the positioning in siglecs (Fig. 4*B*).

Discussion

The PILR pairs are important immune receptors that can deliver opposing cellular signals upon ligand recognition (1). This specific ligand–receptor interaction requires the presence of SA moieties on the ligand surface, drawing parallels between PILRs and siglecs (7, 14). In this study, we report the high-resolution structures of both PILRα and PILRβ, further demonstrating their structural similarities to siglecs. Nevertheless, PILR proteins, unlike siglec molecules, do not exhibit detectable binding for single SA sugar, and their SA-engaging avidity can only been seen in comparative assays with sialylated and desialylated ligands (e.g., HSV-1 gB) (8, 12). How PILRs interact with SA is an interesting issue. Despite great efforts, we were unable to obtain a complex crystal between PILRα and SA. Nevertheless, we successfully turned PILRβ into a gB binder by a single L108W mutation mimicking the PILRα and managed to solve the complex structure between SA and this mutant protein. The revealed binding mode shows that residues Y2, W28, R95, Q107, W108, and Q109 are involved in the SA engagement. These amino acids are exactly the same between PILRα and PILRβ-mut (Fig. S2). Further taking into account the extremely high structural similarity between these two molecules, we infer that PILRα likely uses a binding mode similar to that of PILRβ-mut for SA interaction.

It is interesting that the Y/R/W triresidue is arranged in a linear mode in PILRα. In comparison with this ligand-free structure, an obvious orientation difference in the N-terminal loop and a dramatic conformational variance in the loop-residing tyrosine (Y2) residue are observed in the PILRβ-mut–SA complex structure. This leads again to a triangular arrangement of the triresidue as in siglecs, although in a different manner as described in *Results*. Although it cannot be excluded that the L108W mutation may affect the steric positioning of Y2, this is unlikely the case because PILRα shares with PILRβ-mut exactly the same amino acids for SA binding but arranges the tyrosine residue in an extended conformation. Therefore, the conservation in amino acids constituting the SA-binding site between PILRα and PILRβ-mut seems to favor a possible rearrangement of the N-terminal loop (N loop) and Y2 as a ligand-induced event. Nevertheless, this remains hypothetical because of the lack of structures of either the PILRα–SA complex or the free PILRβ-mut protein, which we have been unable to crystallize so far. Alternatively, it might be an intrinsic character of PILRα with an N loop of certain flexibility. Upon SA binding, the N loop is flipped and further stabilized by the bound SA moiety. In either case, we believe that the formation of an intact SA-binding site in PILRα requires a large shift in Y2 (Fig. 4*C*). In the free PILRα structure, this N loop cannot flip owing to the packing

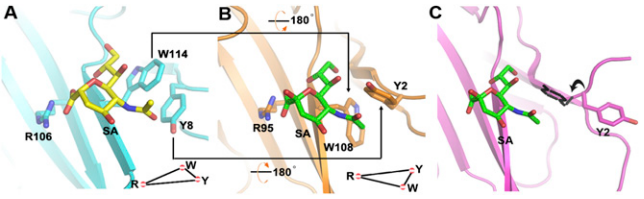

Fig. 4. Comparison of the SA-binding mode between PILRβ-mut and siglecs. Both PILRβ-mut and siglecs use a key triresidue motif for SA engagement. The two aromatic residues of the motif, which rotate their side chains~180° degrees in the PILR protein relative to the individual equivalent amino acids in siglecs, are marked. This leads the triangular arrangement of the triresidue to mirror each other between PILRβ-mut and siglecs, which is highlighted at the bottom with solid-line triangles. (*A*) SA (yellow) bound to siglec-7 (cyan) as a representative. (*B*) SA (green) bound to PILRβ-mut (orange). (*C*) A structural model between PILRα and SA. We believe that the formation of an intact SA-binding site in PILRα requires a large shift (marked with an arrow) in Y2. The observed tyrosine residue in the free PILRα structure is indicated with magenta sticks, and the modeled residue capable of engaging SA is shown as dashed gray sticks. The SA moiety is in green.

mode of the PILRα crystal. We believe the crystal pack obstructs Y2 shift and the PILRα/SA complex formation.

We also developed an effective SPR assay for a quantitative characterization of the PILR–SA interaction. The arginine and tryptophan amino acids of the triresidue are shown to be indispensable in the SA engagement of PILRs. In our complex structure, the arginine residue indeed plays a key role in binding by providing important salt-bridge contacts. Similar interactions have also been observed in siglecs (15, 17, 22). The tryptophan, however, only hydrophobically contacts the N-acetyl methyl of SA. Unlike its siglec counterpart, which is sandwiched between SA and the N-terminal tyrosine/tryptophan via π–π interactions (15, 17, 22), this PILR residue orients its indole ring perpendicularly relative to Y2 and thereby does not support a similar π–π contact as in siglecs. Nevertheless, strong hydrophobic interactions between these two amino acids can still be expected. We noted that Y2 oriented variantly in the ligand-free PILRα structure and in the SA-bound PILRβ-mut structure, and W108 of PILR likely also plays a role in stabilizing Y2 in a conformation suitable for SA interaction. We therefore propose that PILR W108 contributes to the PILR–SA engagement via both a direct and an indirect way, explaining its indispensability in the binding of SA to PILRs. A leucine residue at this position, however, would not be of sufficient size and hydrophobicity to stabilize Y2, thereby precluding PILRβ from interacting with SA.

Few PILRβ ligands have thus far been identified, forming a sharp contrast to its paired partner PILRα, which can be recognized by multiple host and viral molecules (7–10). Mouse CD99 is a natural ligand for mouse PILRβ; specific binding of the two would deliver activating immune signals via the cytoplasmic ITAM motif of the PILR receptor (8). It should be noted that this mouse receptor contains a W108 residue rather than an L108 amino acid as in its human counterpart. Based on our functional and structural data in this study, human PILRβ is unable to interact with SA. Accordingly, human CD99 lacks one of the two *O*-linked glycosylation sites present in mouse CD99 that are indispensable for PILR engagement (7). These observations do not favor a direct interaction between human CD99 and PILRβ, raising questions about whether this human receptor can deliver activating signals similar to those in mice. Alternatively, human PILRβ might use a new yet-unknown mechanism to interact with yet-unidentified molecules for immune activation. This interaction mode might not involve SA. Further studies are needed to settle the issue.

PILRα and PILRβ exhibit a dramatic conformational difference in the CC′ loop. It is notable that these two molecules differ only in a single amino acid (R47/G47) in this loop region. The residue, however, locates at the base of the CC′ loop and is unlikely the reason for the observed conformation variance. We believe the variant CC′ orientation in the PILR pairs possibly reflects a certain extent of flexibility in this loop. In siglecs, the same loop has been shown to be involved in the tuning of the ligand specificity, for which a flexible character would be a prerequisite (19). In accord with this notion, the flexible CC′ loop of PILRs might exert similar functions as an element in fine tuning the ligand specificity.

Multiple host surface molecules have been shown to be exploited by HSV-1 for infection. A major category of the HSV-1 receptor includes herpes virus entry mediator and nectin-1, both of which are recognized by virus gD through specific protein–protein interactions (23–25). PILRα, however, relies on SA binding for the full capacity of gB engagement. Consistently, two *O*-glycosylation sites on gB were demonstrated in a previous study to be of vital importance in this interaction (12). Nevertheless, PILRα is not capable of binding single SA sugars, revealing the possibility of gB combining both SA recognition and amino acid interactions to engage PILRα. This residue-mediated contact could either be independent of or concert with SA-binding. In either case, we believe the contact should be occurring on the accessible surface of the gB trimer [because we used a "crystal form" (26) of gB trimer in the binding study] and might be conserved between PILRα and PILRβ (because we demonstrated that restoring the SA-binding avidity in PILRβ could suffice for the receptor for gB engagement). Nevertheless, we showed in the virus infection assay that PILRβ-mut, with a restored gB-binding capacity, was still unable to function as a coreceptor for HSV-1. This is consistent with a previous study (21) showing that PILRβ with the L108W mutation, unlike PILRα, could not mediate the fusion of CHO-K1 cells expressing PILR with those expressing HSV-1 gD, gB, gH, and gL. The phenomenon favors a possible role of the cytoplasmic and transmembrane domains of PILRα in facilitating the cell entry of HSV-1. It also raises the possibility that PILRβ-mut/SA binding is not reflecting the full features of PILRα–SA interaction or that the receptor specificity is provided by protein–protein contacts between PILRα and gB. The details on the PILRα–gB complex formation requires an atomic costructure, which should be pursued in the future.

Our structural and mutagenesis study delineated the basis for the variant SA-binding avidities between PILRα and PILRβ. It is interesting that HSV-1 has evolved to use this difference to recognize an immuno-inhibitory receptor (PILRα) and to simultaneously avoid binding to its paired activation molecule (PILRβ). Reminiscence of the common occurrence of HSV-1 latency in humans (27), it favors a role of PILR receptors in the HSV virulence. It is also noteworthy that our structures indicate a single SA-binding site in PILRs. The host SA-bearing PILR ligands, such as NPDC1 (7), should be able to compete with gB binding in HSV infection. These are interesting issues worth studying in the future.

Materials and Methods

Protein Preparation. The IgV-domain proteins of human PILRα, PILRβ, and the indicated PILR mutants (PILRα Y2L, R95A, and W108L, as well as PILRβ L108W) were individually expressed as inclusion bodies in *Escherichia coli* cells and then refolded as previously described (28). The refolded proteins were further purified by gel filtration chromatography.

The ectodomain protein of HSV-1 (strain F) gB with an engineered C-terminal 6 his tag was prepared either in Sf9 insect cells or 293T mammalian cells, followed by purification using an Ni-nitrilotriacetic acid HisTrap FF column (GE) and a gel filtration Superose 6 10/300 GL column (GE). The detailed protein-preparation procedures are given in *SI Materials and Methods*.

Protein Characterization. The purified PILR and gB proteins were individually analyzed by an analytical gel filtration assay using calibrated Superdex 75 (10/300 GL) or Superose 6 (10/300 GL) columns. The pooled samples were further analyzed by SDS/PAGE or by Western blot.

Crystallization, Data Collection, and Structure Determination. The initial screening trials were set up with commercial crystallization kits (Hampton Research) using the sitting drop vapor diffusion method. Normally, 1 μL protein was mixed with 1 μL reservoir solution. The resultant drop was then sealed, equilibrating against 100 μL reservoir solution at 4 or 18 °C. After optimization, diffractable crystals were obtained in 0.1 M sodium citrate tribasic dehydrate, pH 5.6, 20% (vol/vol) 2-propanol, and 20% (wt/vol) polyethylene glycol 4,000 for PILRα (4 mg/mL, 4 °C), in 3% (wt/vol) dextran sulfate sodium salt, 0.1 M Bicine, pH 8.5, and 15% (wt/vol) polyethylene glycol 20,000 for PILRβ (8 mg/mL, 18 °C), and in 0.1 M Hepes sodium, pH 7.5, and 1.4 M sodium citrate tribasic dehydrate for the PILRβ-mut–SA complex (5 mg/mL protein mixed in advance with 10 mM SA, 18 °C).

The crystals were first incubated in mother liquor containing 20% (vol/vol) glycerol for cryoprotection and then flash-cooled at 100 K. The heavy atom derivative data for PILRα were obtained from crystals transiently immersed (~30 s) in a cryoprotectant solution containing extra 1 M KI. All of the datasets were collected at the Shanghai Synchrotron Radiation Facility beamline BL17U. The data were processed and scaled using HKL2000 (29). The structure of PILRα was solved by single isomorphous replacement, and the structures of PILRβ and PILRβ-mut–SA complex were solved by molecular replacement method with the structure of PILRα as the search model using

the program MOLREP (30). Initial restrained rigid-body refinement was performed using REFMAC5 (31), which was followed by manual rebuilding and adjustment in COOT (32). Further refinement was carried out using Phenix (33). The stereochemical qualities of the final models were assessed with the program PROCHECK (34). The statistics are provided in Table S1.

SPR Measurements. The binding kinetics of the PILRα, PILRβ, and the mutant PILR forms to gB (gB-293T, gB-Sf9, or gB-NA) were analyzed at 25 °C on a Biacore 3000 machine with CM5 chips (GE Healthcare). HBS-EP buffer (10 mM Hepes, 150 mM NaCl, 3 mM EDTA, and 0.005% Tween-20) was used for all measurements and the blank channel of the chip was used as the negative control. Approximately 1,000 response units of gB were immobilized on the chip, followed by blockade with ethylenediamine. The PILR proteins were then injected at 30 μL/min over the chips. After each cycle, the sensor chip was regenerated with 10 mM NaOH. The analyte concentrations ranged from 0 to 50 μM. Sensorgrams were fit globally with Biacore 3000 analysis software (BIAevaluation version 4.1) using a 1:1 Langumuir binding model and the steady-state affinity algorithm. For each binding pair, the goodness of fit between the calculated model and the experimental data was ascertained by a low χ^2 value.

Confocal Fluorescence Imaging. The full-length coding fragments of PILRα/β and the indicated PILR mutants were individually cloned into pEGFP-N1 vector via the XhoI and BamHI restriction sites. The subsequent plasmids were used to transfect HeLa cells using lipofectamine 2000 (Invitrogen) following the manufacturer's instructions. Twenty-four hours posttransfection, cells were fixed with 4% (wt/vol) paraformaldehyde for 15 min and then washed with PBS. The cells were then treated with 0.2% Triton X-100 for 5 min, stained with DAPI for another 5 min, and thoroughly washed with PBS. The images were obtained with a Zeiss upright confocal microscope (Zeiss LSM 710).

Virus Infection Assay. The virus infection assay was conducted with CHO-K1 cells [selected for absence of PILRα ligands (10)] kindly provided by Hisashi Arase, Osaka University, Osaka and a genetically modified HSV-1 virus containing a luciferase gene (35). The cells were cultured in F-12 medium (Gibco) containing 10% FBS (vol/vol) (Gibco) and transiently transfected with a pcDNA4.0 plasmid or the PILR-expressing (the individual PILR coding sequence subcloned into pcDNA4.0) plasmids or a nectin-1–expressing (the full length nectin-1 coding sequence subcloned into pcDNA4.0) plasmid using Lipofectamine 2000 (Invitrogen). The medium was replaced with F-12 containing 1% FBS 24 h posttransfection, and the cells were cultured for another 24 h before infection. The cells were then collected, mixed with HSV-1 at a *multiplicity of infection* of 10, and centrifuged at 32 °C at 1,100 × *g* for 2 h. After a 24-h incubation, the cells were harvested, washed, and tested for luciferase activity using a Luminometer20/20n (Turner Biosystems). The statistical analysis was performed by GraphPad Prism using the two-tailed Student *t* test with data obtained from three independent experimental replicates.

ACKNOWLEDGMENTS. We thank the staff at the Shanghai Synchrotron Radiation Facility (beamline 17U) and Xiaolan Zhang, Tong Zhao, and Lijun Gu (Institute of Microbiology, Chinese Academy of Sciences) for assistance. This work was supported by the 973 project, China Ministry of Science and Technology Grants 2010CB530104 and 2010CB911902, National Natural Science Foundation of China (NSFC) Grants 31030030 and 31390432, and Strategic Priority Research Program of the Chinese Academy of Sciences Grant XDB08020100. G.F.G. is a Leading Principal Investigator of the Innovative Research Group of the NSFC (Grant 81321063).

1. Wilson MD, Cheung J, Martindale DW, Scherer SW, Koop BF (2006) Comparative analysis of the paired immunoglobulin-like receptor (PILR) locus in six mammalian genomes: Duplication, conversion, and the birth of new genes. *Physiol Genomics* 27(3):201–218.
2. Fournier N, et al. (2000) FDF03, a novel inhibitory receptor of the immunoglobulin superfamily, is expressed by human dendritic and myeloid cells. *J Immunol* 165(3): 1197–1209.
3. Mousseau DD, Banville D, L'Abbé D, Bouchard P, Shen SH (2000) PILRalpha, a novel immunoreceptor tyrosine-based inhibitory motif-bearing protein, recruits SHP-1 upon tyrosine phosphorylation and is paired with the truncated counterpart PILRbeta. *J Biol Chem* 275(6):4467–4474.
4. Tato CM, et al. (2012) The myeloid receptor PILRβ mediates the balance of inflammatory responses through regulation of IL-27 production. *PLoS ONE* 7(3):e31680.
5. Wang J, Shiratori I, Uehori J, Ikawa M, Arase H (2013) Neutrophil infiltration during inflammation is regulated by PILRα via modulation of integrin activation. *Nat Immunol* 14(1):34–40.
6. Shiratori I, Ogasawara K, Saito T, Lanier LL, Arase H (2004) Activation of natural killer cells and dendritic cells upon recognition of a novel CD99-like ligand by paired immunoglobulin-like type 2 receptor. *J Exp Med* 199(4):525–533.
7. Sun YL, et al. (2012) Evolutionarily conserved paired immunoglobulin-like receptor α (PILRα) domain mediates its interaction with diverse sialylated ligands. *J Biol Chem* 287(19):15837–15850.
8. Wang J, Shiratori I, Satoh T, Lanier LL, Arase H (2008) An essential role of sialylated O-linked sugar chains in the recognition of mouse CD99 by paired Ig-like type 2 receptor (PILR). *J Immunol* 180(3):1686–1693.
9. Kogure A, Shiratori I, Wang J, Lanier LL, Arase H (2011) PANP is a novel O-glycosylated PILRα ligand expressed in neural tissues. *Biochem Biophys Res Commun* 405(3): 428–433.
10. Satoh T, et al. (2008) PILRalpha is a herpes simplex virus-1 entry coreceptor that associates with glycoprotein B. *Cell* 132(6):935–944.
11. Arii J, et al. (2009) Entry of herpes simplex virus 1 and other alphaherpesviruses via the paired immunoglobulin-like type 2 receptor alpha. *J Virol* 83(9):4520–4527.
12. Wang J, et al. (2009) Binding of herpes simplex virus glycoprotein B (gB) to paired immunoglobulin-like type 2 receptor alpha depends on specific sialylated O-linked glycans on gB. *J Virol* 83(24):13042–13045.
13. Crocker PR, Paulson JC, Varki A (2007) Siglecs and their roles in the immune system. *Nat Rev Immunol* 7(4):255–266.
14. Tabata S, et al. (2008) Biophysical characterization of O-glycosylated CD99 recognition by paired Ig-like type 2 receptors. *J Biol Chem* 283(14):8893–8901.
15. Zhuravleva MA, Trandem K, Sun PD (2008) Structural implications of Siglec-5-mediated sialoglycan recognition. *J Mol Biol* 375(2):437–447.
16. May AP, Robinson RC, Vinson M, Crocker PR, Jones EY (1998) Crystal structure of the N-terminal domain of sialoadhesin in complex with 3′ sialyllactose at 1.85 A resolution. *Mol Cell* 1(5):719–728.
17. Zaccai NR, et al. (2003) Structure-guided design of sialic acid-based Siglec inhibitors and crystallographic analysis in complex with sialoadhesin. *Structure* 11(5):557–567.
18. Alphey MS, Attrill H, Crocker PR, van Aalten DMF (2003) High resolution crystal structures of Siglec-7. Insights into ligand specificity in the Siglec family. *J Biol Chem* 278(5):3372–3377.
19. Attrill H, et al. (2006) Siglec-7 undergoes a major conformational change when complexed with the alpha(2,8)-disialylganglioside GT1b. *J Biol Chem* 281(43): 32774–32783.
20. Lopez M, et al. (1999) O-glycosylation potential of lepidopteran insect cell lines. *Biochim Biophys Acta* 1427(1):49–61.
21. Fan Q, Longnecker R (2010) The Ig-like v-type domain of paired Ig-like type 2 receptor alpha is critical for herpes simplex virus type 1-mediated membrane fusion. *J Virol* 84(17):8664–8672.
22. Attrill H, et al. (2006) The structure of siglec-7 in complex with sialosides: leads for rational structure-based inhibitor design. *Biochem J* 397(2):271–278.
23. Zhang N, et al. (2011) Binding of herpes simplex virus glycoprotein D to nectin-1 exploits host cell adhesion. *Nat Commun* 2:577.
24. Di Giovine P, et al. (2011) Structure of herpes simplex virus glycoprotein D bound to the human receptor nectin-1. *PLoS Pathog* 7(9):e1002277.
25. Carfí A, et al. (2001) Herpes simplex virus glycoprotein D bound to the human receptor HveA. *Mol Cell* 8(1):169–179.
26. Heldwein EE, et al. (2006) Crystal structure of glycoprotein B from herpes simplex virus 1. *Science* 313(5784):217–220.
27. McLennan JL, Darby G (1980) Herpes simplex virus latency: The cellular location of virus in dorsal root ganglia and the fate of the infected cell following virus activation. *J Gen Virol* 51(Pt 2):233–243.
28. Zhang S, et al. (2013) Competition of cell adhesion and immune recognition: Insights into the interaction between CRTAM and nectin-like 2. *Structure* 21(8):1430–1439.
29. Otwinowski Z, Minor W (1997) Processing of X-ray diffraction data collected in oscillation mode. *Methods Enzymol* 276:307–326.
30. Vagin A, Teplyakov A (1997) MOLREP: An automated program for molecular replacement. *J Appl Cryst* 30:1022–1025.
31. Murshudov GN, Vagin AA, Dodson EJ (1997) Refinement of macromolecular structures by the maximum-likelihood method. *Acta Crystallogr D Biol Crystallogr* 53(Pt 3): 240–255.
32. Emsley P, Cowtan K (2004) Coot: Model-building tools for molecular graphics. *Acta Crystallogr D Biol Crystallogr* 60(Pt 12 Pt 1):2126–2132.
33. Adams PD, et al. (2010) PHENIX: A comprehensive Python-based system for macromolecular structure solution. *Acta Crystallogr D Biol Crystallogr* 66(Pt 2):213–221.
34. Laskowski RA, Macarthur MW, Moss DS, Thornton JM (1993) Procheck - a program to check the stereochemical quality of protein structures. *J Appl Cryst* 26:283–291.
35. Li Y, Wang S, Zhu H, Zheng C (2011) Cloning of the herpes simplex virus type 1 genome as a novel luciferase-tagged infectious bacterial artificial chromosome. *Arch Virol* 156(12):2267–2272.